

Spin-correlation functions of the $S = 1$ Heisenberg-Ising chain by the large-cluster-decomposition Monte Carlo method

Kiyohide Nomura

Institute for Solid State Physics, University of Tokyo, Roppongi, Minato-ku, Tokyo 106, Japan

(Received 5 June 1989)

We study the spin-correlation functions of the one-dimensional $S=1$ antiferromagnetic Heisenberg-Ising model by the large-cluster-decomposition Monte Carlo method. It is found that this model shows a second-order transition at the anisotropy parameter $\lambda_c = 1.167 \pm 0.007$. The obtained critical exponents ($\eta = 0.253 \pm 0.002$, $\beta = 0.126 \pm 0.007$, $\nu = 0.98 \pm 0.02$) strongly suggest that this transition belongs to the same universality class as the two-dimensional Ising model.

I. INTRODUCTION

The one-dimensional (1D) Heisenberg-Ising model

$$H = \sum_i (S_i^x S_{i+1}^x + S_i^y S_{i+1}^y + \lambda S_i^z S_{i+1}^z) \quad (1.1)$$

has attracted much attention, both theoretical and experimental. In the case of $S = \frac{1}{2}$, many properties of the ground state are well known.¹⁻³ Between the antiferromagnetic (AF) ($\lambda > 1$) and the ferromagnetic (F) phase ($\lambda < -1$), there exists an XY phase, characterized by a gapless ground state¹ and a power-law decay of the spin-correlation functions.² Approaching from the AF region to the isotropic point ($\lambda = 1$), this model shows essential singularity, the energy gap and the staggered magnetization vanish as³

$$\Delta \sim \exp[-C(\lambda - 1)^{-1/2}] . \quad (1.2)$$

Haldane⁴ took the continuum limit of the XXZ model, and found that this model can be mapped onto the O(3) nonlinear σ model in 1+1 dimensions. From this analogy he argued that, in the case of the integer spin, this model shows different behavior from the $S = \frac{1}{2}$ case. The gapless XY phase for $\lambda < \lambda_1$ ($0 \leq \lambda_1 < 1$) and the ordered AF phase for $\lambda > \lambda_2$ ($1 < \lambda_2$) are still present, but a new phase appears for $\lambda_1 < \lambda < \lambda_2$. This novel phase has an energy gap and its correlation function decays exponentially. For the half-integer case, there appears an additional topological term to the nonlinear σ model, and its phase diagram is similar to the $S = \frac{1}{2}$ case.

Much work has been done to examine this conjecture, using numerical diagonalization⁵⁻⁹ and the Monte Carlo method.¹⁰⁻¹⁴ Botet and Jullien⁵ carried out an exact diagonalization of finite systems. Their analysis by the finite-size-scaling technique supports Haldane's prediction. But this result is criticized by Bonner and Müller,⁶ and independently by Sólyom and Ziman.⁷ Bonner and Müller applied the finite-size-scaling technique to the $S = \frac{1}{2}$ case, and they concluded that a system size up to $N = 30$ might be required to find the true asymptotic finite-size behavior. The existence of the energy gap was confirmed by a Monte Carlo simulation of Nightingale and Blöte.¹⁰ They calculated the lowest energies of

$\sum_i S_i^z = 0$ and $\sum_i S_i^z = 1$ subspace, and they concluded that the energy gap is $0.41J$ in the limit of $N \rightarrow \infty$. Takahashi calculated the elementary excitation using the projector Monte Carlo method.¹³ He found that the spectra for $S = \frac{1}{2}$ and $S = 1$ are completely different. The former has the shape $c|\text{sinc}|$, while the latter has the shape $c(\sin^2 k + \xi^{-2})^{1/2}$. In a previous paper¹⁴ we carried out a Monte Carlo simulation of this system, and found that the correlation function decays as

$$|l|^{-1/2} \exp(-l/\xi), \quad 1/\xi = 0.160 ,$$

which is consistent with Haldane's conjecture.

In this paper, we investigate the correlation function of this model by the large-cluster-decomposition Monte Carlo method.¹⁴⁻¹⁸ It was found that the transition point between the AF and singlet phase is located at $\lambda_2 = 1.167 \pm 0.007$, and the critical exponents are very close to those of the two-dimensional (2D) Ising model.

II. METHOD

We write the antiferromagnetic Heisenberg Hamiltonian as follows:

$$H = \sum_{i=0}^{N-1} h_i ,$$

$$h_i = S_i^x S_{i+1}^x + S_i^y S_{i+1}^y + \lambda S_i^z S_{i+1}^z , \quad (2.1)$$

$$S_N = S_0 .$$

Using the large-cluster decomposition,¹⁴⁻¹⁸ which is a variant of the pair-decomposition Monte Carlo method,¹⁹ we get the following equation for the partition function Z :

$$Z \simeq \text{Tr}(V_1 V_2)^L ,$$

$$V_1 = \prod_{k=\text{odd}} \exp(-\tau H_k) ,$$

$$V_2 = \prod_{k=\text{even}} \exp(-\tau H_k) , \quad (2.2)$$

$$H_k = \sum_{j=0}^{p-1} h_{pk+j} ,$$

$$\tau = \beta/L ,$$

where p is a cluster size (see Fig. 1). A Monte Carlo state is represented by a set of $N \times 2L$ classical spins $S_{i,j}^z (i=0, \dots, N-1, j=0, \dots, 2L-1)$. The Boltzman weight is given by

$$\mathcal{W}(\{S_{i,j}^z\}) = \prod_{k+j=\text{even}} \langle \alpha_{k,j} | \exp(-\tau H_k) | \alpha_{k,j+1} \rangle, \quad (2.3)$$

$$|\alpha_{k,j}\rangle \equiv |S_{pk,j}^z, S_{pk+1,j}^z, \dots, S_{p(k+1),j}^z\rangle.$$

In a Monte Carlo trial, we employ the two types of updating processes, the inner block process and corner process. These processes must satisfy local spin conservation,

$$\sum_{i=1}^p S_{pk+i,j}^z = \sum_{i=0}^p S_{pk+i,j+1}^z \quad (k+j=\text{even}), \quad (2.4)$$

and the following identity:

$$S_{pk+i,j+1}^z = S_{pk+i,j+2}^z \quad (k+j=\text{even}, i=1, \dots, p-1). \quad (2.5)$$

These processes are illustrated in Fig. 2. In the inner block process, we choose the new states $\{S_{i,j}^z\}$ which satisfy

$$\sum_{i=1}^{p-1} S_{pk+i,j}^z = \sum_{i=1}^{p-1} S_{pk+i,j}^z,$$

$$S_{pk+i,j+1}^z = S_{pk+i,j}^z \quad (i=1, \dots, p-1), \quad (2.6)$$

$$|S_{i,j}^z| \leq S,$$

$$S_{pk,j}^z = S_{pk,j}^z, \quad S_{p(k+1),j}^z = S_{p(k+1),j}^z \quad (k+j=\text{odd}),$$

and we accept one of the states using the heat-bath method. Similarly, in the left-corner process, we choose new states $\{S_{i,j}^z\}$ which satisfy

$$S_{pk,j}^z = S_{pk,j}^z + m,$$

$$S_{pk,j+1}^z = S_{pk,j+1}^z + m,$$

$$S_{pk+1,j}^z = S_{pk+1,j+1}^z = S_{pk+1,j}^z - m,$$

$$|S_{i,j}^z| \leq S \quad (k+j=\text{odd}, m=\text{integer}) \quad (2.7)$$

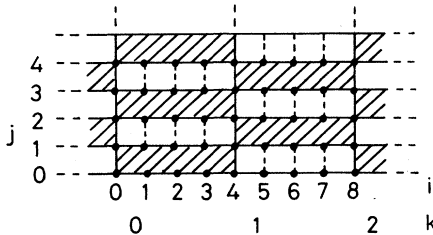


FIG. 1. Graphical representation of the p -spin cluster decomposition in the case of $p=4$. The equivalent classical lattice is represented by a checkerboard-like lattice; i denotes sites on the original 1D lattice, k is a label of the spin cluster p , and j is a label along the Trotter direction. The shaded rectangles denote where $2(p+1)$ local spins interact. The two spins on the sites connected by the dashed lines are equal.

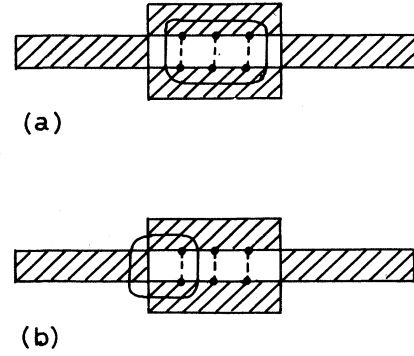


FIG. 2. (a) The inner block process. (b) The corner process. The encircled spins are flipped.

and we accept one of the states using the heat-bath method. The right-corner process can be done in the same way.

In the case of the pair-decomposition Monte Carlo method, if one reduces τ to include sufficient quantum effects, the acceptance of the new states decreases, and the longer Monte Carlo steps are needed to reach thermal equilibrium.²⁰ Using the large-cluster decomposition, one can take account of the quantum effects for fairly large τ .

The correlation function of the quantum system is given by

$$p(l) \equiv N^{-1} \sum_i \langle S_i^z S_{i+l}^z \rangle$$

$$= (2NL)^{-1} \sum_{i,j} \langle S_{imj}^z S_{i+l,j}^z \rangle. \quad (2.8)$$

In order to calculate the correlation function, following Takahashi,¹² we use the structure factor $S(q)$

$$S(q) \equiv \sum_l e^{iql} \rho(l) = (2L)^{-1} \sum_{j=0}^{2L-1} \langle |S_{q,j}^z|^2 \rangle,$$

$$S_{q,j}^z = N^{-1/2} \sum_m e^{iqm} S_{m,j}^z. \quad (2.9)$$

In the sequence of the Monte Carlo simulation we calculate $S(q)$ by the fast Fourier transformation. After the Monte Carlo calculation of $S(q)$, we calculate $\rho(l)$ by the inverse Fourier transformation. Using this method, the speed of the calculation is faster than the conventional method ($N \log_2 N$ versus N^2).

III. RESULTS

A. Critical exponents

We have dealt with the cases $N=64$, $\tau=0.5$, and $\beta=32$, which can be regarded, practically, as zero temperature. And we set the cluster size $p=4$. The ratio of the inner block and the corner processes is chosen as 4:1. After the 2×10^5 Monte Carlo steps thermalization, we did eight runs with 10^5 Monte Carlo steps. We investigate only $\sum_{i=0}^{N-1} S_{i,j}^z = 0$ subspace, because we are mainly

interested in the ground state. We do not employ the global process to change the winding number because system size is large enough that the contribution from this process is negligibly small.

We calculate the longitudinal correlation function $\rho(l) = \langle S_0^z S_l^z \rangle$. In Fig. 3 we show the log-log plot of the spin-correlation functions at various anisotropy. Above $\lambda \geq 1.20$, this model seems to have the long-range order. The staggered magnetization M_s is evaluated according to

$$M_s^2 = \lim_{l \rightarrow \infty} |\langle S_0^z S_l^z \rangle|. \quad (3.1)$$

We analyze the staggered magnetization near the critical point in the form

$$M_s = C|\lambda - \lambda_c|^\beta, \quad (3.2)$$

and we obtain (see Fig. 4)

$$\begin{aligned} C &= 1.01 \pm 0.02, \\ \beta &= 0.126 \pm 0.007, \\ \lambda_c &= 1.172 \pm 0.004. \end{aligned} \quad (3.3)$$

As we have found in a previous paper,¹⁴ the correlation function of the isotropic Heisenberg model is well described by the 2D Orstein-Zernike form, that is, the modified Bessel function. In the singlet phase ($\lambda \leq 1.15$), we approximate the longitudinal correlation function in the form

$$|\rho(l)| = AK_0(l/\xi), \quad (3.4)$$

where ξ denotes the correlation length. As will be seen later, this assumption is asymptotically correct [see Eq. (3.12)]. The correlation length ξ and the amplitude A of Eq. (3.4) are assumed to behave as

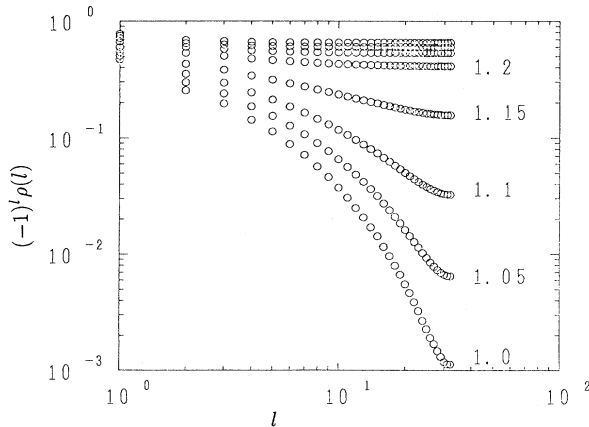


FIG. 3. Spin-correlation functions $(-1)^l \rho(l)$ are plotted as a function of l in a log-log plot. Anisotropy parameters are taken as $\lambda = 1.00, 1.05, 1.10, 1.15, 1.20, 1.25, 1.30$, and 1.35 . Correlation functions for the $\lambda \leq 1.15$ behavior are qualitatively different from $\lambda \geq 1.20$. The latter seems to have the long-range order.

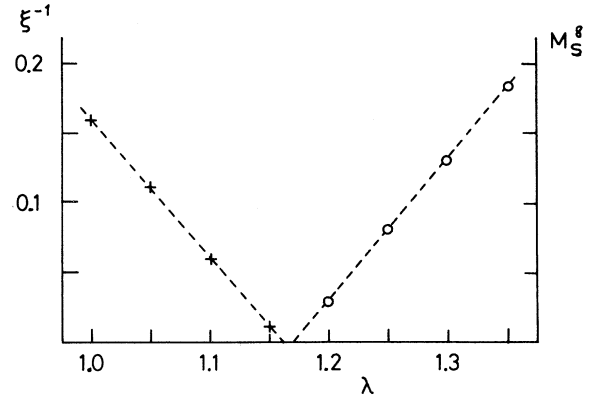


FIG. 4. Staggered magnetization M_s and correlation length ξ as a function of λ . (\circ) M_s ; ($+$) ξ .

$$\begin{aligned} \xi &= C|\lambda - \lambda_c|^{-\nu}, \\ A &= C'|\lambda - \lambda_c|^{\eta'}. \end{aligned} \quad (3.5)$$

We estimate ξ and A from the data $l = 6-16$ using Eq. (3.4), and we obtain (see Fig. 4)

$$\begin{aligned} C &= 1.05 \pm 0.03, \\ C' &= 0.31 \pm 0.02 \simeq \pi^{-1}, \\ \lambda_c &= 1.162 \pm 0.004, \\ \nu &= 0.98 \pm 0.02, \\ \eta' &= 0.25 \pm 0.03. \end{aligned} \quad (3.6)$$

From Eqs. (3.3) and (3.6), we can conclude $\lambda = 1.167 \pm 0.007$.

The correlation function at the critical point λ_c behaves like

$$|\rho(l)| = A|l|^{-\eta}. \quad (3.7)$$

We obtain from the data $l = 6-10$ (see Fig. 5)

$$A = 0.554 \pm 0.002, \quad \eta = 0.253 \pm 0.002. \quad (3.8)$$

These values of the critical exponents are very close to those of the classical 2D Ising model ($\eta = \frac{1}{4}$, $\nu = 1$, $\beta = \frac{1}{8}$), when we regard the variable $\lambda - \lambda_c$ as $T - T_c$.

B. Scaling properties

From the results of previous section we can assume that the correlation function $\rho(l)$ has the following scaling property:

$$\rho(l) = |\lambda - \lambda_c|^{1/4} f_{\pm}(|\lambda - \lambda_c|l), \quad (3.9)$$

where $f_{\pm}(x)$ is the scaling function. The $+$ ($-$) refers to $\lambda < \lambda_c$ ($\lambda > \lambda_c$). In Fig. 6 we plot $|\lambda - \lambda_c|^{-1/4} |\rho(l)|$ as a function of $|\lambda - \lambda_c|l$. Except for the data near the critical point, $|\lambda - \lambda_c|^{-1/4} |\rho(l)|$ shows the scaling behavior beautifully.

As is well known,²¹ the correlation function of the 2D

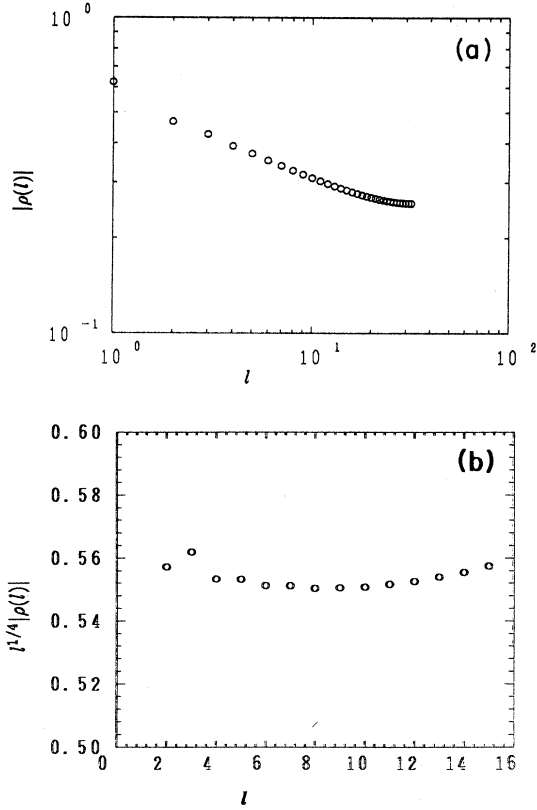


FIG. 5. Spin-correlation function $|\rho(l)|$ at the critical point $\lambda_c = 1.167$ is plotted as a function of l . (a) the log-log plot. (b) $l^{1/4}|\rho(l)|$.

Ising model is asymptotically described by

$$\langle \sigma_{0,0} \sigma_{M,N} \rangle \simeq R^{-1/4} F_{\pm}(t), \quad (3.10)$$

where

$$\begin{aligned} t &\simeq R|\beta - \beta_c|4E, \\ R &= (M^2 + N^2)^{1/2}, \end{aligned} \quad (3.11)$$

and E is the coupling constant of the 2D Ising model.

As $t \rightarrow \infty$,

$$F_{+}(t) = 2^{1/8} (2t)^{1/4} \pi^{-1} K_0(t) + O(e^{-3t}), \quad (3.12)$$

and

$$\begin{aligned} F_{-}(t) &= 2^{1/8} (2t)^{1/4} \{ 1 + \pi^{-2} [t^2 [K_1^2(t) - K_0^2(t)] \\ &\quad - t K_0(t) K_1(t) \\ &\quad + \frac{1}{2} K_0^2(t)] \} + O(e^{-4t}). \end{aligned} \quad (3.13)$$

Conversely, as $t \rightarrow 0$,

$$\begin{aligned} F_{\pm}(t) &= 2^{1/8} e^{1/4} 2^{1/2} A^{-3} [1 \pm \frac{1}{2} t \Omega + \frac{1}{16} t^2 \pm \frac{1}{32} t^3 \Omega \\ &\quad + \frac{1}{256} t^4 (-\Omega^2 + \Omega + \frac{1}{8}) \\ &\quad + O(t^5 \Omega^4), \end{aligned} \quad (3.14)$$

$$\Omega = \ln(t/8) + \gamma_E,$$

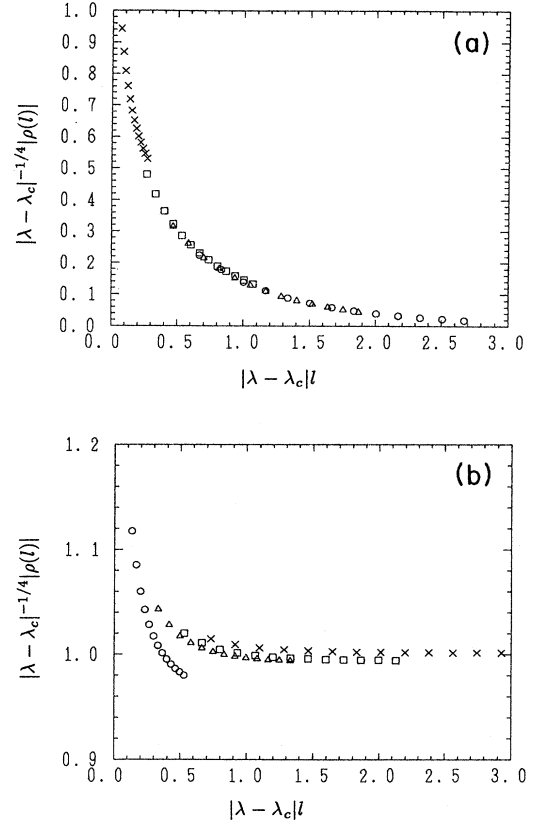


FIG. 6. $|\lambda - \lambda_c|^{-1/4} |\rho(l)|$ as a function of $|\lambda - \lambda_c|l$. Here the data $l = 4-16$ are shown. (a) $\lambda \leq \lambda_c$: (\circ) $\lambda = 1.00$, (\triangle) $\lambda = 1.05$, (\square) $\lambda = 1.10$, (\times) $\lambda = 1.15$. (b) $\lambda \geq \lambda_c$: (\circ) $\lambda = 1.20$, (\triangle) $\lambda = 1.25$, (\square) $\lambda = 1.30$, (\times) $\lambda = 1.35$.

where

$$\gamma_E = 0.57721566490153 \dots$$

is Euler's constant, and

$$A = 1.28242712910062 \dots$$

is Glaisher's constant.

If we assume the form of the scaling function as Eq. (3.10), it is found that the correlation function $|\rho(l)|$ is well described by

$$\begin{aligned} f(l) &= R^{-1/4} F_{\pm}(t) 2^{-1/8} 2^{-1/4} \times (1.02 \pm 0.03), \\ t &= |\lambda - \lambda_c|l \times (1.00 \pm 0.02). \end{aligned} \quad (3.15)$$

In Fig. 7 we plot $|\rho(l)|/f(l)$ at various anisotropies. Except for the data near the critical point where the correlation length ξ diverges, the correlation function $|\rho(l)|$ agrees with $f(l)$ within a few percent. This fact also supports that this transition belongs to the same universality class as the 2D Ising model.

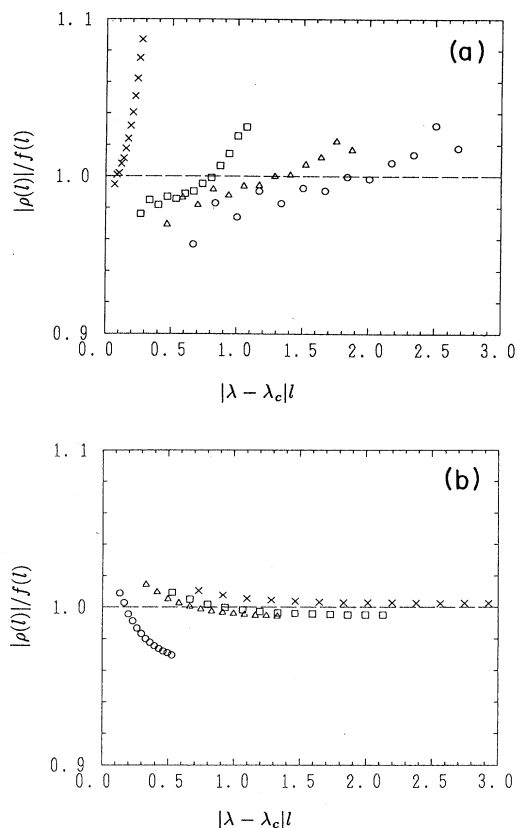


FIG. 7. $|\rho(l)|/f(l)$. Function $f(l)$ is defined by Eq. (3.15). Here the data $l=4-16$ are shown. The meanings of the symbols are same as Fig. 6. (a) $\lambda \leq \lambda_c$. (b) $\lambda \geq \lambda_c$.

IV. DISCUSSION

We find that the 1D $S=1$ Heisenberg-Ising model shows a second-order transition. The obtained critical point and critical exponents are

$$\begin{aligned} \lambda_c &= 1.167 \pm 0.007, \\ \nu &= 0.98 \pm 0.02, \\ \beta &= 0.126 \pm 0.007, \\ \eta &= 0.253 \pm 0.002. \end{aligned} \quad (4.1)$$

These exponents strongly suggest that this transition belongs to the same universality class as the 2D Ising model. This critical behavior is drastically different from the $S=\frac{1}{2}$ case, which shows essentially singularity at the Heisenberg point [cf. Eq. (1.2)]. Our result is consistent with Haldane's prediction that this transition is the Onsager ϕ^4 -field-theory type.⁴

We also find that the correlation function is very well described by the same scaling function as the 2D Ising model, except for the data near the critical point. Since, in our simulation, both system size and β are finite ($N=64$, $\beta=32$), physical properties in the region where the correlation length diverges are not well described.

Botet and Jullien⁵ analyzed this system by the finite-size scaling technique. They have found that

$$\begin{aligned} \lambda_c &= 1.18 \pm 0.01, \\ \nu &= 1.3 \pm 0.2, \\ \beta &= 0.17 \pm 0.05, \\ \eta &= 0.23 \pm 0.03. \end{aligned} \quad (4.2)$$

Their results are different from ours. We think that this difference comes from the fact that they treated rather small systems (system size up to $N=12$) to reach the true asymptotic finite-size behavior.

ACKNOWLEDGMENTS

I wish to thank Professor M. Takahashi for fruitful discussion. Numerical calculations were performed by S-820 in the computer center at the University of Tokyo.

- ¹H. A. Bethe, Z. Phys. **71**, 205 (1931); C. N. Yang and C. P. Yang, Phys. Rev. **151**, 258 (1966).
- ²A. Luther and I. Peschel, Phys. Rev. B **12**, 3908 (1975).
- ³R. J. Baxter, J. Phys. C **6**, L94 (1973).
- ⁴F. D. M. Haldane, Phys. Rev. Lett. **50**, 1153 (1983); Phys. Lett. **93A**, 464 (1983).
- ⁵R. Botet and R. Jullien, Phys. Rev. B **27**, 613 (1983); R. Botet, R. Jullien, and M. Kolb, *ibid.* **28**, 3914 (1983); M. Kolb, R. Botet, and R. Jullien, J. Phys. A **16**, L673 (1983).
- ⁶J. C. Bonner and G. Müller, Phys. Rev. B **29**, 5216 (1984).
- ⁷J. Sólyom and T. A. L. Ziman, Phys. Rev. B **30**, 3980 (1984).
- ⁸A. Moreo, Phys. Rev. B **35**, 8562 (1987); Y. Natsume and M. Matsushita (unpublished).
- ⁹J. B. Parkinson and J. C. Bonner, Phys. Rev. B **32**, 4703 (1985).
- ¹⁰M. P. Nightingale and H. W. Blöte, Phys. Rev. B **33**, 659 (1986).
- ¹¹K. Sogo and M. Uchinami, J. Phys. A **19**, 493 (1986); M. Uchinami, Phys. Lett. A **127**, 151 (1988).
- ¹²M. Takahashi, Phys. Rev. B **38**, 5188 (1988).
- ¹³M. Takahashi, Phys. Rev. Lett. **62**, 2313 (1989).
- ¹⁴K. Nomura, Phys. Rev. B **40**, 2421 (1989).
- ¹⁵T. Tsuzuki, Prog. Theor. Phys. **73**, 1352 (1985); **75**, 225 (1986).
- ¹⁶H. Betsuyaku, Prog. Theor. Phys. **75**, 774 (1986).
- ¹⁷Y. Okabe and M. Kikuchi, J. Phys. Soc. Jpn. **56**, 1963 (1987).
- ¹⁸K. Nomura and M. Takahashi, J. Phys. Soc. Jpn. **57**, 1424 (1988).
- ¹⁹M. Barma and B. S. Shastry, Phys. Lett. **61A**, 15 (1977); Phys. Rev. B **18**, 3351 (1978); J. E. Hirsch, R. L. Sugar, D. J. Scalapino, and R. Blankenbecler, *ibid.* **26**, 5033 (1982).
- ²⁰A. Wiesler, Phys. Lett. **89A**, 359 (1982).
- ²¹T. T. Wu, B. M. McCoy, C. A. Tracy, and E. Barouch, Phys. Rev. B **13**, 316 (1976).